Nanofluid flow and heat transfer in a thin film on a Stretching Sheet with multishapes of Silver Nanoparticles

Azeem Shahzad*¸ Saima Rani*, Ramzan Ali**

*Basic Sciences Department, University of Engineering and Technology, Taxila, 47050, Pakistan
(Azeem.shahzad@uettaxila.edu.pk, saimarani089@gmail.com,)
**Department of Mathematics and Natural Sciences, University of Central Asia, Naryn, Kyrgyz Republic
(alian.qau@gmail.com.

Abstract: *Under boundary condition, the present study manipulates the unsteady film flow and heat transfer of Ag water nanofluid over a stretching sheet. Over a stretching surface, the influence of flow slip on the nanofluid boundary layer is investigated. The current findings provide a foundation for understanding the impact of the slip boundary condition on nanofluid heat and mass transfer beyond stretching sheets. The governing equations are transformed into a system of ordinary differential equations using the similarity transformation method. The BVP4C program numerically evaluates these equations as well as the boundary conditions.*
Keywords: *Thin film; Shape factor; Convective boundary condition; Ag-nanofluid; Heat transfer*

I.   Introduction

Since the concept of dispersing nanoscale particles into a fluid was first presented in the late twentieth century, the topic of nanofluids has gotten a lot of attention. The rising number of studies on nanofluids published each year demonstrates this. Nanofluids are gaining popularity due to their improved thermophysical properties and potential to be implemented into a wide range of thermal applications, from improving the efficiency of industrial heat exchangers to solar energy harvesting for renewable energy production. The use of nanoscale particles to improve the thermal properties of these fluids has created a new form in the study of heat transfer fluids. The suspension of these solid particles in the base fluid improves energy transmission in the fluid, resulting in enhanced thermal conductivity and heat transfer qualities [1]. The thermal conductivity of the resulting fluids has been found to be greater [2,3]. Nanofluids were named for the first time by Choi and Eastman. Nanofluids are colloidal suspensions of nanoscale particles (10--100 nm) in a base fluid that have been manufactured [4]. Metals, metallic oxides, and other carbon-based elements are commonly found in these particles. The number of papers concerning nanofluids since 2010 demonstrates the increased emphasis on nanofluids research over the last decade.

Norio Taniguchi, a Japanese researcher, was the first to present Nanotechnology [5]. Over time, this science's use spread to a variety of sectors, including material sciences, electronics, and biology [6]. As nanoparticles span the gap between bulk materials and atomic or molecular structures, they are of tremendous scientific interest [7]. Metal nanoparticles are the most promising of all nanoparticles, owing to their antibacterial capabilities, which are caused by their high surface to volume ratio. The physical and chemical properties of nanoparticles can bechanged by changing the size or surface of the composition [8]. Metal nanoparticles have been used extensively in recent decades because of their numerous applications in a variety of sectors [9]. The physical, chemical, and electrical properties of nanoparticles change when they reach a certain size range (1--100 nm). These qualities are determined by the size and form of silver nanoparticles, and attributes like as melting temperature, magnetic behavior, redox potential, and color can be manipulated by altering their size and shape [10]. Due to their high conductivity, chemical stability, usage as catalysts [11], and uses in different industries, including the medical sciences, silver nanoparticles have gained a lot of attention in recent years. In order to combat the HIV virus, food manufacturers use antibacterial compounds[12] in food packing [13], as well as their distinctive electrical and optical capabilities [14].

Heat transfer enhancement of nanofluids has been proposed in recent years as a means of outperforming present heat transfer rates in liquids [15]. A nanofluid is a fluid in which solid nanoparticles with nanometer-scale length scales are suspended in a traditional heat transfer fluid. It has been established that adding highly conductive particles to a pure base fluid can considerably improve its thermal conductivity. For example, at 0.3 percent volume of dispersed particles, the effective thermal conductivity of an ethylene--glycol-based nanofluid containing nano size copper particles with diameters smaller than 10 nm improved by up to 40 [16]. [17,18] as well as Das et al. book's [19], provide a thorough overview of nanofluid physics and advancements. The current expe-

rimental evidence reveals that in the presence of nanoparticles, force-convection improves [20], and that the enhancement rises as the nanoparticle volume fraction increases [21].

In nanotechnology, silver nanoparticles (Ag NP) are a significant advancement. Silver nanoparticles are useful for a wide range of applications due to their unique physicochemical and antibacterial properties. Biomedicines, medical equipment, functional textiles, cosmetics, food packaging, food supplements, odour-resistant products, electronics, household appliances, dental amalgam, water disinfectants, paints, and room sprays are among the most common. As a result, the manufacturing of silver nanoparticles has increased in response to rising demand. In 2009, the overall estimated output of silver nanoparticles was around 500 tones per year, with an increase of nearly 900 tones expected by 2025.

Shape	Name
	Sphere
	Brick
	Cylinder
	Platelet
	Blade

Silver nanoparticles (AgNPs) are a type of material with diameters ranging from 1 to 100 nanometers. Because of their unique and appealing physical, chemical, and biological features, there has recently been a rise in interest in studying AgNPs and their diverse behaviour. Toxicity, surface plasmon resonance, and electrical resistance are all recognized to be distinctive features of AgNPs. On the basis of these findings, extensive research has been carried out to determine their qualities and possible applications for a variety of reasons, including antimicrobial agents in wound dressings, anticancer agents, electronic devices, and water treatment [22].

Table 1: Thermo-physical characteristics of base fluid and Ag nanoparticle [23]

Nanoparticle and Base fluid	Thermal Conductivity (W/mK)	Density (Kg/m^3)	Electrical Conductivity (S/m)	Specific heat (J/KgK)
Ag	429	10500	63	235
H_2O	0.613	997.19	5.50	4179

Table2: Shape factor and Viscosity values of nanoparticles [24]

Nanoparticle's Shape	A1	A2	m
Platelet	37.1	612.6	5.72
Cylinder	13.5	904.4	4.82
Blade	14.6	123.3	8.26
Brick	1.9	471.4	3.72
Sphere	2.5	6.5	3.0

II.   Numerical Solution

The goal of this work is to investigate the unsteady flow of Ag nanofluid in a thin layer across a stretching sheet coupled to a slit. In a rectangular coordinate system, the stretchy flat sheet is taken along the x-axis and the y-axis is normal to the sheet. The thin film flow is created by stretching the sheet along the x-axis with velocity $U_w = \frac{bx}{1-\alpha t}$, while   temperature distribution at the wall is given by:

$$T_s = T_0 - T_r \left(\frac{bx^2}{2v_f}\right)(1 - \alpha t)^{-3/2}$$

where b and a are the dimensional constants. T_r and T_0 denote the constant reference and split temperatures, respectively, whereas v_{f} specifies the fundamental fluid's kinematic viscosity. The uniform magnetic field described by $B(t) = \frac{B_0}{\sqrt{1-\alpha t}}$ works perpendicular to the stretching layer, as shown in Figure 1.
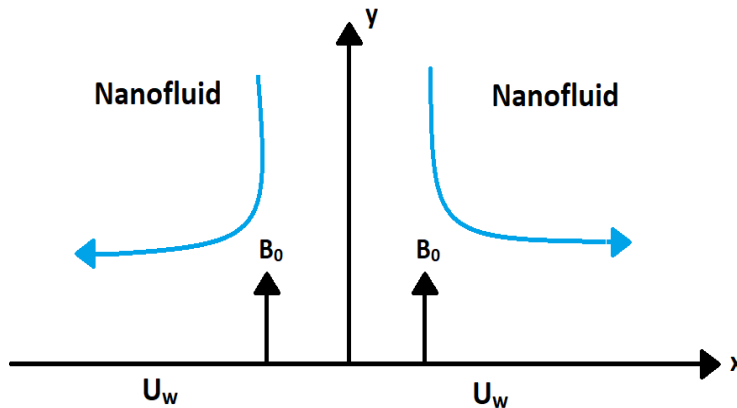
Figure 2. Geometry of the flow problem.

Let *u = u(x, y, t)*   and *v = v(x, y, t)* be the velocity components across the coordinate axes, and *T = T(x, y, t)* be the temperature of the nanofluid. Let the base fluid (water) and nanoparticles of various shapes to be thermally balanced as well. Based on these assumptions and the proposed nanofluid model [25]. In addition to the equations for continuity, there are also equations for momentum and energy [26],

$$\frac{\partial u}{\partial x} + \frac{\partial v}{\partial y} = 0, \tag{1}$$

$$\frac{\partial u}{\partial t} + u\frac{\partial u}{\partial x} + v\frac{\partial u}{\partial y} = \frac{\mu_{nf}}{\rho_{nf}}\frac{\partial^2 u}{\partial y^2} - \frac{\sigma_{nf}}{\rho_{nf}}uB^2(t), \tag{2}$$

$$\frac{\partial T}{\partial t} + u\frac{\partial T}{\partial x} + v\frac{\partial T}{\partial y} = \alpha_{nf}\frac{\partial^2 T}{\partial y^2} + \frac{\mu_{nf}}{\rho_{nf} C_p}\left(\frac{\partial u}{\partial y}\right)^2. \tag{3}$$

following are the boundary conditions

,

$$u = U_w + A_{vf}\frac{\partial u}{\partial y}, T_s = T_0 \text{ at } y = 0 \tag{4}$$

$$u = 0, T_0 = T \text{ at } y = \infty \tag{5}$$

Where A is the constant of proportionality. The thermo-physical parameters of the nanofluid/ hybrid nanofluid specified in [27,28], such as density ρ_{nf}, dynamic viscosity μ_{nf}, electrical conductivity σ_{nf}, diffusivity α_{nf}, and heat capacity $(\rho C_p)_{nf}$, are symbolically expressed as

$$\alpha_{nf} = \frac{k_{nf}}{(\rho C_p)_{nf}}, \qquad \rho_{nf} = (1-\phi)\rho_f + \phi\rho_s,$$
$$\mu_{nf} = \mu_f(1 + A_1\phi + A_2\phi^2), \quad \sigma_{nf} = \sigma_f(1-\phi) + \phi\sigma_s),$$
$$(\rho C_p)_{nf} = (1-\phi)(\rho C_p)_f + \phi(\rho C_p)_s, \tag{6}$$

and

$$\frac{k_{nf}}{k_f} = \frac{k_s + (m-1)k_f + (m-1)(k_s - k_f)\phi}{k_s + (m-1)k_f - (k_s - k_f)\phi} \tag{7}$$

The heat capacitance coefficients for viscosity augmentation are A_1, A_2 and $(\rho C_p)_{nf}$ is the coefficient of heat strength, where ϕ is the volume fraction of the nanofluid. The thermal conductivity and shape factor of the nanoparticles are denoted by k_s and m, while the subscripts f, nf and s reflect the thermo-physical properties, respectively, of solid base fluid, nanofluid and nanoparticles.

Table 2 also includes the viscosity enhancement coefficient values A_1, A_2 and the shape factor m for Ag nanofluid multi-form nanoparticles, which are applied to examine numerical and graphical simulations in this report. where the similarity transformations are

$$\eta = [\frac{b}{\nu_f(1 - \alpha t)}]^{1/2}y,$$

$$\psi = [\frac{b\nu_f}{1 - \alpha t}]^{1/2}xf(\eta), \qquad T = T_0 - T_r\left(\frac{bx^2}{2\nu_f}\right)(1 - \alpha t)^{-3/2}\theta(\eta) \tag{8}$$

where stream function ψ determine the pattern of flow and is defined as $u = \frac{\partial \psi}{\partial y}$ and $v = -\frac{\partial \psi}{\partial x}$.

so that equation of continuity is satisfied identically. By substituting the above defined dimensionless variables equation (8) into equations $(2-3)$, the following nonlinear ODEs are obtained. Also, by using (8) in $(4-5)$ the transformed boundary conditions become

$$\varepsilon_1 f'''(\eta) - M\varepsilon_3 f'(\eta) + f(\eta)f''(\eta) - f'^2(\eta) - S\left(f'(\eta) + \frac{\eta}{2}f''(\eta)\right) = 0, \tag{9}$$

$$\frac{\varepsilon_2}{Pr}\theta''(\eta) + \varepsilon_1 f''^2(\eta).Ec - \frac{S}{2}\left(3\theta(\eta) + \eta\theta'(\eta)\right) - 2\theta(\eta)f'(\eta) + \theta'(\eta)f(\eta) = 0, \tag{10}$$

and

$$f(0) = 0, \ f'(0) = 1 + Kf''(0), \ f'(\beta) = 0, \theta(0) = 1 \text{at } \eta = 0,$$

$$f'(\infty) = 0, \theta(\infty) = 0 \text{1at } \eta = \infty. \tag{11}$$

The dimensionless constants $K = A\sqrt{\frac{\nu_f U_w}{x}}, Ec = \frac{U_w^2}{C_p(T_s - T)}, M = \frac{\sigma_f B_0^2}{\rho_{nf} b}, \qquad P_r = \frac{(\rho C_p)_f \nu_f}{k_f}$ and $S = \frac{a}{b}$ are slip parameter, biot-number, Eckert number, magnetic parameter, unsteadiness parameter and Prandtl number respectively. Additionally, $\varepsilon_i, \ i = 1,\dots,3$ are constants and described as

$$\varepsilon_1 = \frac{1 + A_1\phi + A_2\phi^2}{1 - \phi + \phi(\frac{\rho_s}{\rho_f})}, \qquad \varepsilon_2 = \frac{\frac{k_{nf}}{k_f}}{1 - \phi + \phi\frac{(\rho C_p)_s}{(\rho C_p)_f}}, \qquad \varepsilon_3 = \frac{1 - \phi + \phi(\frac{\sigma_s}{\sigma_f})}{1 - \phi + \phi(\frac{\rho_s}{\rho_f})}. \tag{12}$$

where ϕ is the solid volume-fraction. Skin shear stress and heat transfer coefficient are described as

$$C_f = \frac{\tau_w}{\rho_f U_w^2} \quad \text{and} \quad Nu = \frac{q_w x}{k_f(T_s - T_0)},$$

where

$$\tau_w = \mu_{nf}\left(\frac{\partial u}{\partial y}\right)_{y=0} \quad \text{and} \quad q_w = -k_{nf}\left(\frac{\partial T}{\partial y}\right)_{y=0}. \tag{13}$$

The non-dimensionalize form of equation (13) with respect to transformed variables is

$$C_f Re^{1/2} = (1 + A_1\phi + A_2\phi^2)f''(0), \quad NuR_e^{-1/2} = -\frac{k_{nf}}{k_f}\theta'(0). \tag{14}$$

III.   Solutions of the problem

Several researchers have proposed various strategies for solving a nonlinear system, including Kellor box, shooting, and finite difference methods (9-11). The BVP4C technique is proposed in this study as a method for determining the solution to such a system. The BVP4C framework can be viewed as either a C_1 piece-wise cubic polynomial S(x) or an implicit Runge Kutta formula with a continuous (interpolant) extension. A well-known Simpson's scheme is a basic BVP4C approach that can be found in several codes. In addition, [29,30] contains a detailed discussion of BVP4C, as well as error and convergence analysis. Significant aspects of the proposed BVP4C technique include faster convergence with minimal error, direct consideration of not only two-point but multi-point BVPs for higher precision and dealing with singular BVPs in the research directions [31--35].In order to discover the numerical solution to the first-order linear equations, the set of linear first-order equations is obtained.

$$y_1 = f, y_1^{'} = y_2, y_2^{'} = y_3, \tag{15}$$

$$y_3^{'} = \frac{\varepsilon_3}{\varepsilon_1} + My_2 - \frac{1}{\varepsilon_1}\left[y_1 y_3 - y_2^2 - S\left(y_2 + \frac{\eta}{2}y_3\right)\right], \tag{16}$$

$$\theta = y_4, y_4^{'} = y_5, y_5^{'} = -\frac{\varepsilon_1}{\varepsilon_2}PrEcy_3^2 - \frac{1}{\varepsilon_1}\left[y_1 y_3, -2y_4 y_2 - \frac{S}{2}(3y_4 + \eta y_5)\right], \tag{17}$$

$$y_1(0) = 0, y_2(0) = 1 + Ky_3(0), y_4(0) = 1, \tag{18}$$

$$y_2(\infty) = 0, y_4(\infty) = 0. \tag{19}$$

IV.   Numerical results and discussion

Five various shapes of Ag nanoparticles are placed into ordinary base fluid water that are cylinder, platelet, brick, blade, and sphere. Various graphs are used to study the physics of the situation, and the contained parameters are examined in depth. Table 2 is used to select the constants A_1 and A_2. It is worth noting that the form of the particles has a big impact on the coefficients A_1 and A_2. The influence of the unsteadiness parameter S, slip parameter K, volume fraction parameter φ, Prandtl number Pr and Eckert number Ec on the dimensionless temperature profile is depicted in these diagrams. The influence of the unsteadiness parameter S on temperature profile is seen in Fig 3. It has been shown that when the value of S increases, the temperature profile decreases. The influence of the slip parameter K on temperature profile is seen in Fig 4. It has been shown that when the value of K increases, the temperature profile also increases. The influence of the volume fraction parameter φ on temperature profile is seen in Fig 5. It has been shown that increasing the value of φ increases the temperature profile. The influence of Eckert number Ec on temperature profile is seen in Fig 6. It has been shown that increasing the value of Ec increases the temperature profile. The influence of the Prandtl number Pr on temperature profile is seen in Fig 7. It has been shown that when the value of Pr increases, the temperature profile decreases.
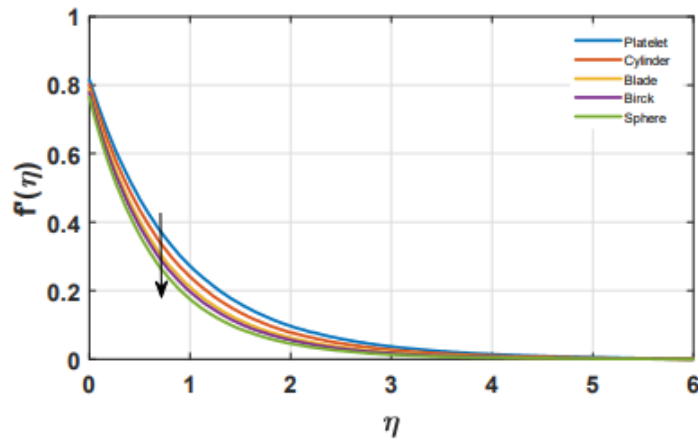
Figure 2. The impact of shape shape onn $f'(\eta)$, for $\varphi = 0.02, S = 0.4, K = 0.5$.
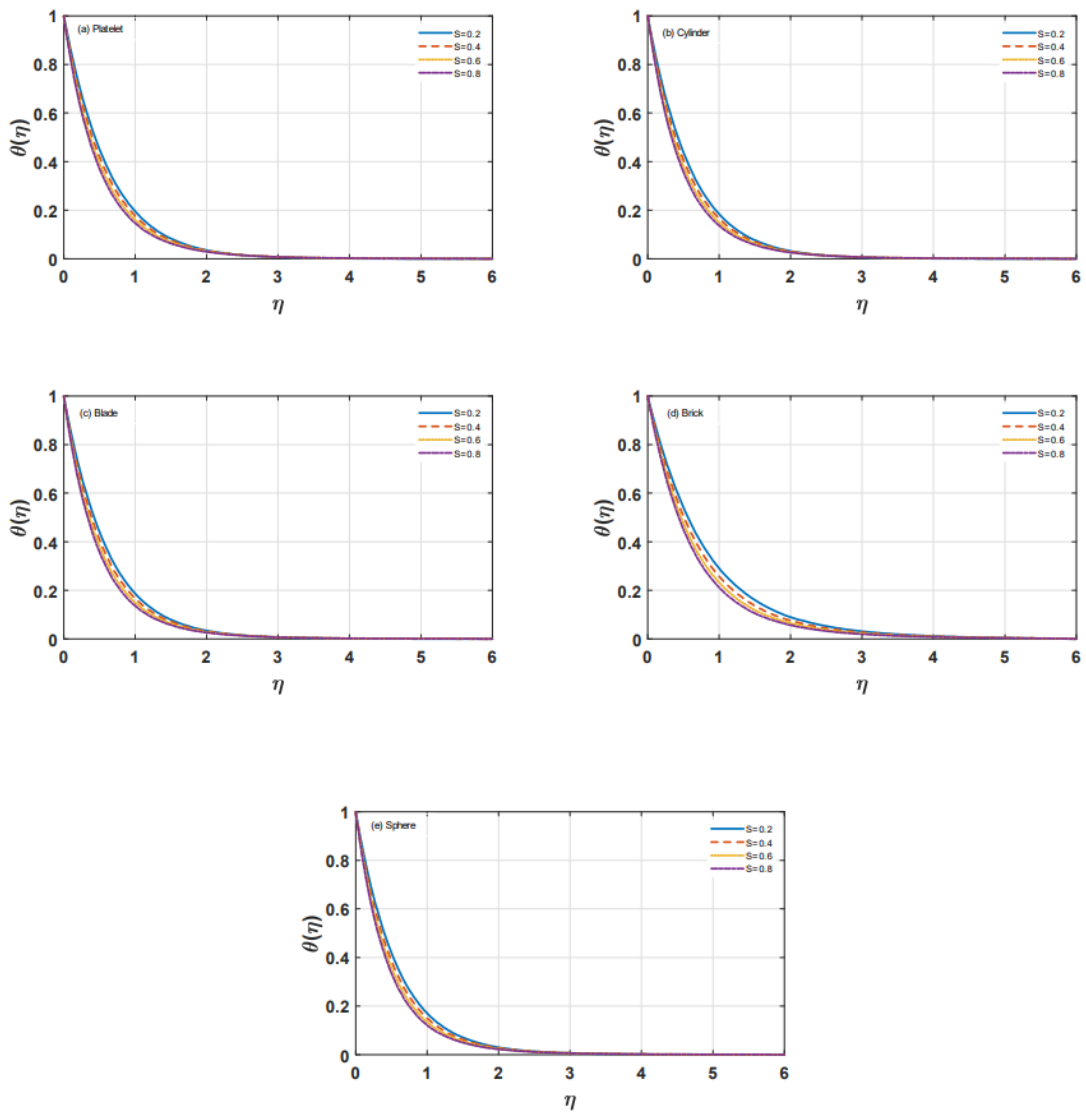
Figure 3. The impact of unsteadiness parameter$S$ on$\theta(\eta)$, for $K = 0.2, \phi = 0.02, Ec = 1.0, Pr = 4.0$.
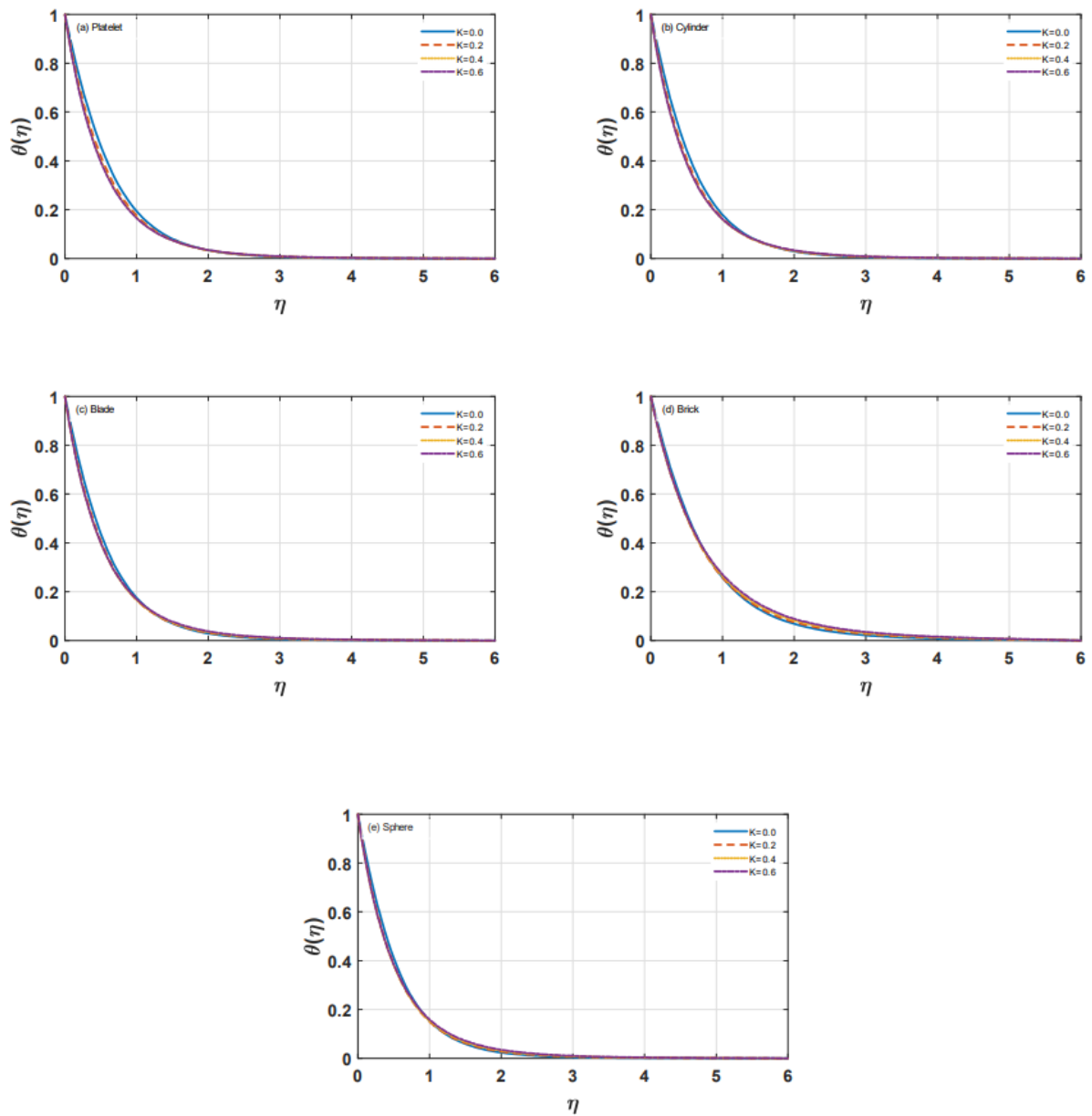
Figure 4. The impact of slip parameter$K$ on $\theta(\eta)$, when $Pr = 0.4$, $\phi = 0.02, S = 0.4, Ec = 1.0$.
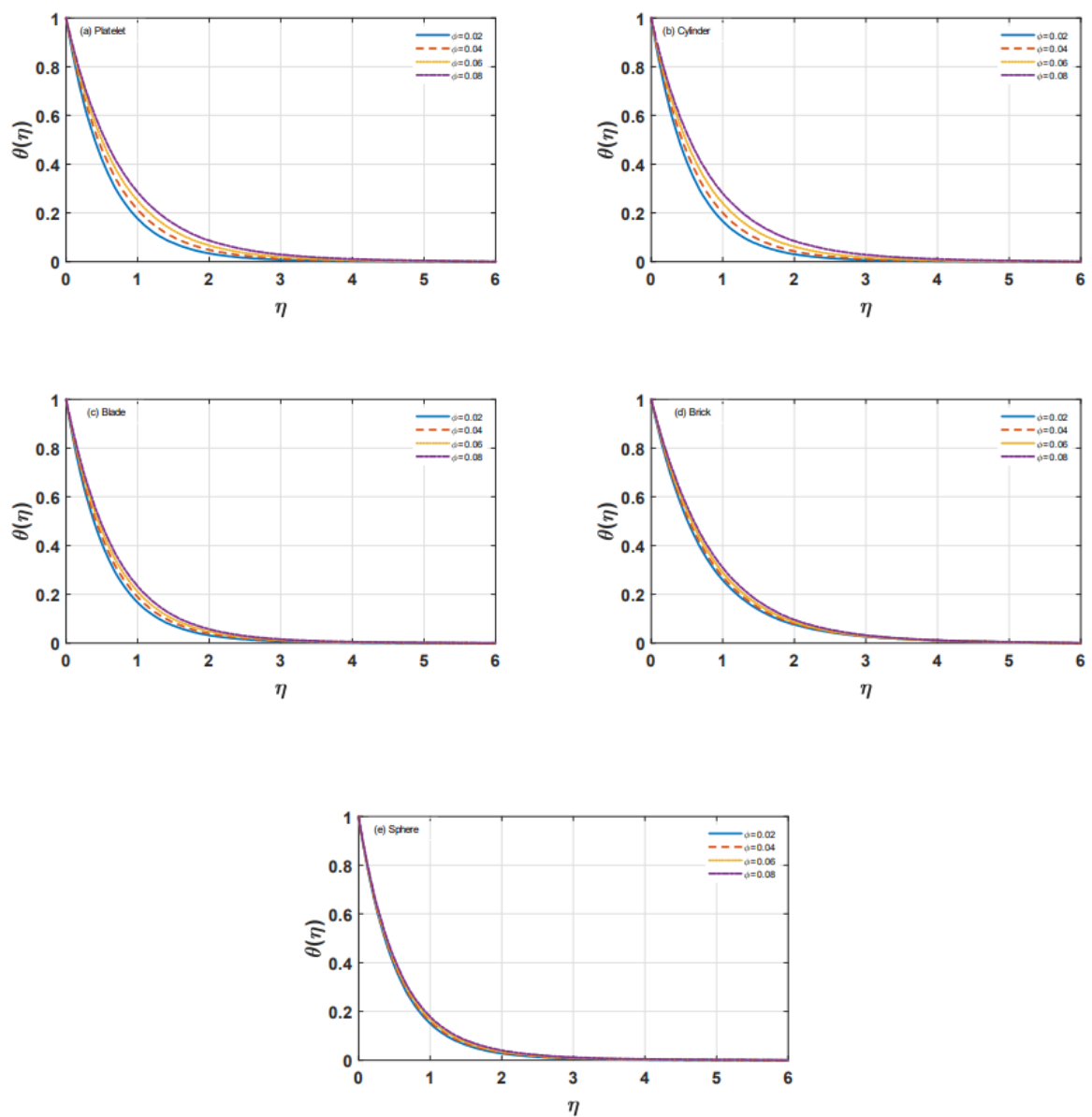
Figure 5. The impact of nanoparticle volume fractionϕ on $\theta(\eta)$ for $K = 0.2$, $Pr = 6.0$, $Ec = 1.0$, $S = 0.4$, $Pr = 4.0$.
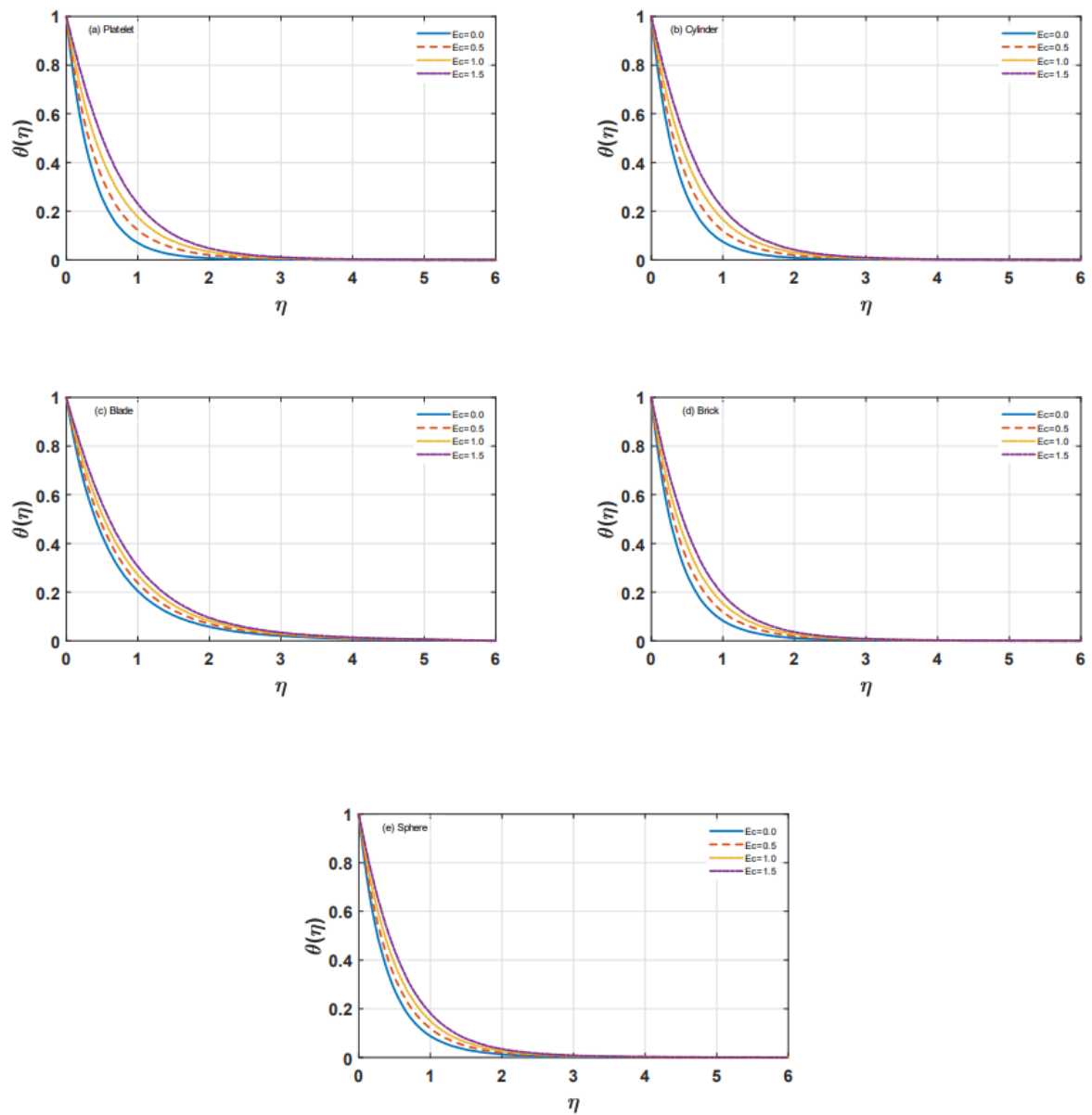
Figure 6. The impact of Ec on $\theta(\eta)$ for $S = 0.4, K = 0.5, \varphi = 0.02, Pr = 6.0$.

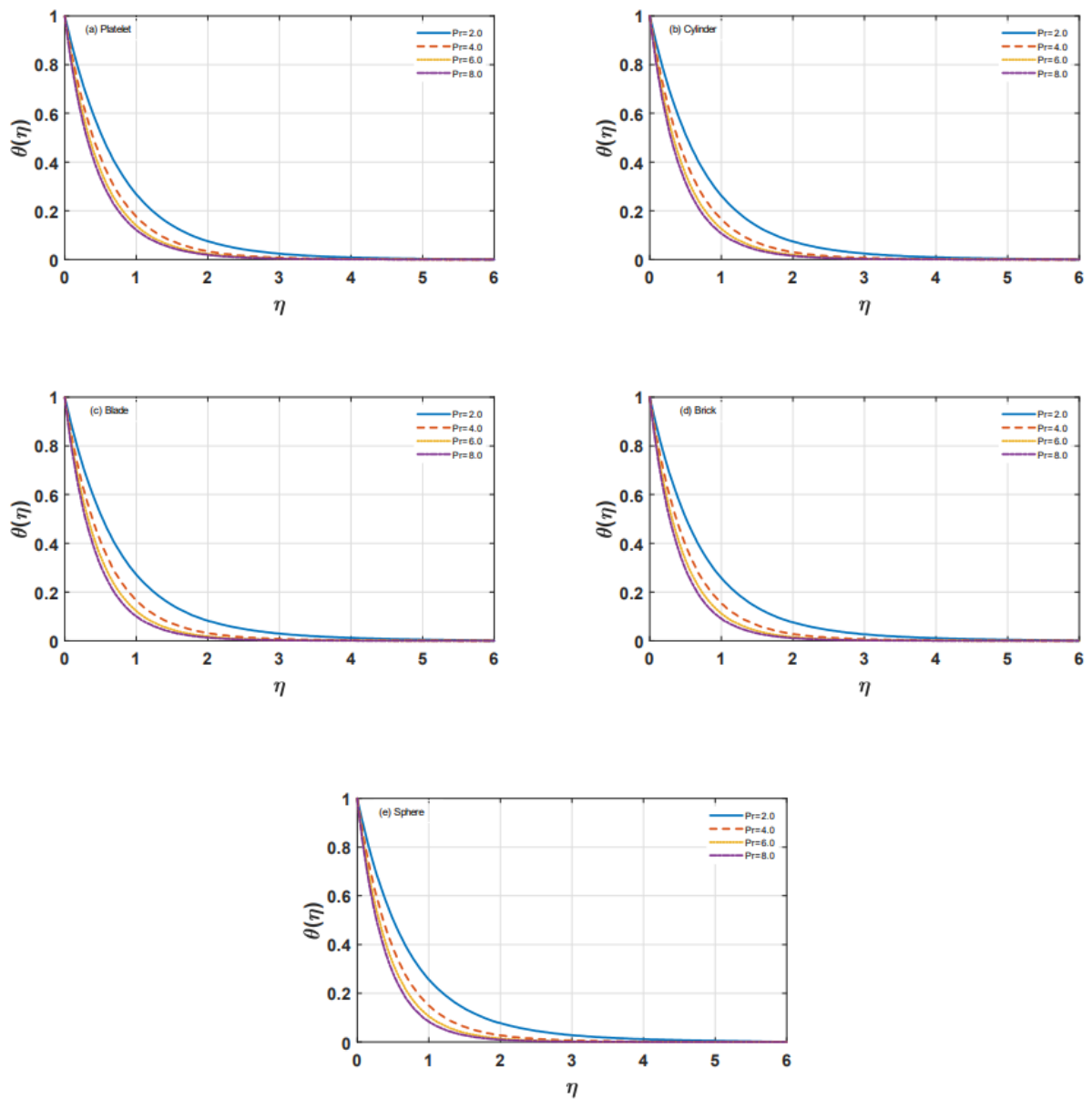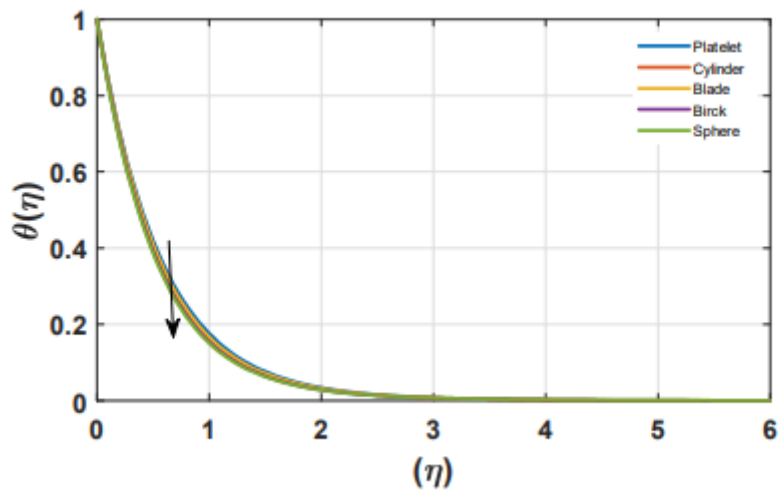**Figure 7.**The impact of Pr on $\theta(\eta)$, for $K = 0.5, S = 0.4, \phi = 0.02, Ec = 1.0$.

Figure 8. The influence of shape factor on temperature profile, for $\phi = 0.02, K = 0.2, S = 0.4, Pr = 4.0, Ec = 1.0$.

The numerical results of dimensionless skin-friction coefficient for different shape of nanoparticles are given in table 3. Decreasing values of skin-friction coefficient are found for increasing values of slip parameter K and unsteadiness parameter S, whereas the reverse behaviour is noticed in case of magnetic parameter M and volume-fraction parameter φ.

Table 3. The skin-friction coefficient's numerical values for multi-shaped nanoparticles.

Physical Parameter				$-Re^{1/2}C_f$				
S	M	K	ϕ	Platelets	Cylinder	Blade	Brick	Sphere
0.2				1.7784106	1.5776437	1.3981824	1.3225037	1.2014794
0.4				1.8299657	1.6227951	1.4376474	1.3595845	1.234768
0.6				1.8797711	1.666365	1.4756849	1.3953039	1.2668023
0.8				1.9278712	1.7083962	1.5123367	1.4297032	1.2976227
	0.0			1.4142485	1.2570655	1.1165844	1.0573219	0.96249379
	1.0			1.8299657	1.6227951	1.4376474	1.3595845	1.234768
	2.0			2.1317442	1.885962	1.6666472	1.574295	1.4267992
	3.0			2.3724207	2.0946378	1.8471319	1.74303	1.5769414
		0.0		2.3375867	2.1183028	1.9205453	1.8365487	1.7013337
		0.2		1.8299657	1.6227951	1.4376474	1.3595845	1.234768
		0.4		1.5146462	1.3260842	1.159409	1.0897325	0.9791568
		0.6		1.2969632	1.1256952	0.97563572	0.91332305	0.81499702
			0.02	1.8299657	1.6227951	1.4376474	1.3595845	1.234768
			0.04	2.7146249	2.4859777	1.8171593	1.8477683	1.3511789
			0.06	3.7336123	3.5851521	2.2499616	2.5282819	1.468467
			0.08	4.8682299	4.8609555	2.7309269	3.3554119	1.5883788

Table 4. The numerical results Nusselt number $-\theta'(0)$ for multi-shape nanoparticles.

Physical Parameter					$Re^{-1/2} Nu$				
S	K	ϕ	Pr	Ec	Platelets	Cylinder	Blade	Brick	Sphere
0.2					1.724452	1.7533821	1.8537467	1.7880134	1.7983801
0.4					1.9263452	1.9567787	2.0683897	1.9950644	2.0076651
0.6					2.1114863	2.1430933	2.2643485	2.1840429	2.1981113
0.8					2.283145	2.3157533	2.4456102	2.3588332	2.3739762
	0.2				1.5509665	1.5861838	1.702428	1.6366323	1.6585224
	0.4				1.9263452	1.9567787	2.0683897	1.9950644	2.0076651
	0.6				2.0769625	2.0901316	2.1826411	2.1009783	2.0980474
	0.8				2.1393612	2.1375368	2.2136772	2.126615	2.1123674
		0.02			1.9263452	1.9567787	2.0683897	1.9950644	2.0076651
		0.04			1.9134146	1.9237449	2.1903338	2.0088545	2.0749379
		0.06			1.9074778	1.8827616	2.3048293	2.0010185	2.1383399
		0.08			1.9089699	1.8483516	2.4144246	1.9873318	2.1989962
			2.0		1.4250449	1.4367644	1.5043698	1.448726	1.4493363
			4.0		1.9263452	1.9567787	2.0683897	1.9950644	2.0076651
			6.0		2.2838373	2.3288235	2.4735163	2.3882632	2.410996
			8.0		2.5724716	2.6295003	2.8012272	2.7067066	2.7381342
				0.0	3.1151442	3.0448289	3.0787357	2.9440099	2.8848135
				0.5	2.5207447	2.5008038	2.5735627	2.4695371	2.4462393
				1.0	1.9263452	1.9567787	2.0683897	1.9950644	2.0076651
				2.0	1.3319457	1.4127536	1.5632168	1.5205916	1.5690909

V. Concluding Remarks

A numerical simulation of heat transfer of a thin film flow through nanofluids on an unsteady stretching surface is examined. The impact of various shapes of Ag nanoparticles on the temperature of nanofluids, such as platelets, blades, cylinders, bricks, and spheres of equal volume, has been calculated with varying results. Nanofluid viscosity and thermal conductivity are influenced by particle shape, volume fraction, and base fluid. The flow parameters' behaviour is observed. The following is a summary of the current work.

- It has been shown that when the value of S increases, the temperature profile decreases
- It has been shown that when the value of K increases, the temperature profile also increases.
- It has been shown that increasing the value of φ increases the temperature profile
- It has been shown that increasing the value of Ec increases the temperature profile.
- It has been shown that when the value of Pr increases, the temperature profile decreases.
- The Ag nanofluid velocity and temperature profile is approaching its maximum and minimum on platelet and sphere-shapednanoparticles.

References
[1]. D. D. Ganji, Y. Sabzehmeidani, amd A. Sedighiamiri, Nonlinear systems in heat transfer (2018) Elsevier.
[2]. E. C. Okonkwo, I. Wole-Osho, D. Kavaz, and M. Abid, Comparison of experimental and theoretical methods of obtaining the thermal properties of alumina/iron mono and hybrid nanofluids. Journal of Molecular Liquids, (2019).292,111377.
[3]. S. U. Choi, and J. A. Eastman, Enhancing thermal conductivity of fluids with nanoparticles (No. ANL/MSD/CP-84938; CONF-951135-29). Argonne National Lab., IL (United States). (1995).
[4]. P. Sivashanmugam, Application of nanofluids in heat transfer. An overview of heat transfer phenomena, (2012)16.

[5]. J. P. Abid, A. W. Wark, P. F. Brevet, and H. H. Girault, Preparation of silver nanoparticles in solution from a silver salt by laser irradiation. Chemical Communications, (2002)(7),792-793.
[6]. M. A. Aguilar-Méndez, E. San Martín-Martínez, L. Ortega-Arroyo, G. Cobián-Portillo, and E. Sánchez-Espíndola, Synthesis and characterization of silver nanoparticles: effect on phytopathogen Colletotrichum gloesporioides. Journal of Nanoparticle Research, (2011)13(6),2525-2532.
[7]. D. Aherne, D. M. Ledwith, M. Gara, and J. M. Kelly, Optical properties and growth aspects of silver nanoprisms produced by a highly reproducible and rapid synthesis at room temperature. Advanced Functional Materials, (2008)18(14),2005-2016.
[8]. A. Ahmad, P. Mukherjee, S. Senapati, D. Mandal, M. I. Khan, R. Kumar, and M. Sastry, Extracellular biosynthesis of silver nano-particles using the fungus Fusarium oxysporum. Colloids and surfaces B: Biointerfaces, (2003)28(4),313-318.
[9]. S. A. AL-Thabaiti, M. A. Malik, A. A. Al-Youbi, Z. Khan, and J. I. Hussain, Effects of surfactant and polymer on the morphology of advanced nanomaterials in aqueous solution. Int. J. Electrochem. Sci, (2013)8(1),204-218.
[10]. T. Peter Amaladhas, T. Akkini Devi, N. Ananthi, S. Priya Velammal, and S. Sivagami, Biogenic synthesis of silver nanoparticles by leaf extract of Cassia angustifolia. Advances in Natural Sciences. Nanoscience and Nanotechnology (Online), (2012)3.
[11]. A. A. Ashkarran, A novel method for synthesis of colloidal silver nanoparticles by arc discharge in liquid. Current Applied Physics, (2010)10(6),1442-1447.
[12]. V. Bastys, I. Pastoriza-Santos, B. Rodríguez-González, R. Vaisnoras, and L. M. Liz-Marzán, Formation of silver nanoprisms with surface plasmons at communication wavelengths. Advanced Functional Materials, (2006)16(6),766-773.
[13]. K. Aslan, J. R. Lakowicz, and C. D. Geddes, Rapid deposition of triangular silver nanoplates on planar surfaces: application to metal-enhanced fluorescence. The Journal of Physical Chemistry B, (2005)109(13),6247-6251.
[14]. J. S. Bhat, Heralding a new future--Nanotechnology?. Current Science, (2003)85(2),147-154.
[15]. N. A. Yacob, A. Ishak, I. Pop, and K. Vajravelu, Boundary layer flow past a stretching/shrinking surface beneath an external uniform shear flow with a convective surface boundary condition in a nanofluid. Nanoscale research letters, (2011)6(1),1-7.
[16]. J. A. Eastman, S. U. S. Choi, S. Li, W. Yu, and L .J. Thompson, Anomalously increased effective thermal conductivities of ethylene glycol-based nanofluids containing copper nanoparticles. Applied physics letters, (2001)78(6),718-720.
[17]. W. Daungthongsuk, and S. Wongwises, A critical review of convective heat transfer of nanofluids. Renewable and sustainable energy reviews, (2007)11(5),797-817.
[18]. V. Trisaksri, and S. Wongwises, Critical review of heat transfer characteristics of nanofluids. Renewable and sustainable energy reviews, (2007)11(3),512-523.
[19]. S. K Das, S. U. Choi, W. Yu, and T. Pradeep, Nanofluids: science and technology. John Wiley and Sons. (2007).
[20]. K. Wongcharee, and S. Eiamsa-Ard, Enhancement of heat transfer using CuO/water nanofluid and twisted tape with alternate axis. International Communications in Heat and Mass Transfer, (2011)38(6),742-748.
[21]. K. S. Hwang, S. P. Jang and S. U. Choi, Flow and convective heat transfer characteristics of water-based Al2O3 nanofluids in fully developed laminar flow regime. International journal of heat and mass transfer, (2009)52(1-2),193-199.
[22]. N. H. Mthombeni, L. Mpenyana-Monyatsi, M. S. Onyango and M. N. Momba, Breakthrough analysis for water disinfection using silver nanoparticles coated resin beads in fixed-bed column. Journal of hazardous materials, (2012)217,133-140.
[23]. E. V. Timofeeva, J. L. Routbort and D. Singh, Particle shape effects on thermo-physical properties of alumina nanofluids, Journal of Applied Physics, (2009)106(1), 014304
[24]. S. R. Vajjha and K. D. Debendra, Experimental determination of thermal conductivity of three nanofluids and development of new correlations. International Journal of Heat and Mass Transfer, (2009)52(21-22),4675-4682.
[25]. R. J. Tiwari, and M. K. Das, Heat transfer augmentation in a two-sided lid-driven differentially heated square cavity utilizing na-nofluids, International Journal of Heat and Mass Transfer, (2002-2018)50,(9-10).
[26]. Fakour et al. Nanofluid thin film flow and heat transfer over an unsteady stretching elastic sheet by LSM, Journal of Mechanical Science and Technology, (2018)32 (1),177-183.
[27]. Vanaki et al. Effect of nanoparticle shapes on the heat transfer enhancement in a wavy channel with different phase shifts, Journal of Molecular Liquids, 196(2014),32-42.
[28]. R. L. Hamilton and O. K. Crosser, Thermal conductivity of heterogeneous two component systems, Industrial & Engineering Che-mistry Fundamentals, 1(3)(1962),187-191.
[29]. L. F. Shampine et al, Solving boundary value problems for ordinary differential equations in MATLAB with bvp4c, Toturial Notes, 2000(2000),1-27.
[30]. J. Kierzenka, Studies in the numerical solution of ordinary differential equations, PhD Thesis, Southern Methodist University, Dallas, TX, (1998).
[31]. J. Ahmed, M. Khan and L. Ahmad, Stagnation point flow of Maxwell nanofluid over a permeable rotating disk with heat source/sink. Journal of Molecular Liquids, 287(2019),110853.
[32]. K. Naganthran, I. Hashim and R. Nazar, Triple solutions of Carreau thin film flow with thermocapillarity and injection on an unsteady stretching sheet. Energies, (2020)13(12),3177.erials, 493, p.165646.
[33]. A Shahzad, R Ali, M Khan, On the exact solution for axisymmetric flow and heat transfer over a nonlinear radially stretching sheet, Chinese Physics Letters 29 (8), 084705
[34]. A Farooq, R Ali, AC Benim, Soret and Dufour effects on three dimensional Oldroyd-B fluid, Physica A: Statistical Mechanics and its Applications 503, 345-354.
[35]. A Shahzad, R Ali, Approximate analytic solution for magneto-hydrodynamic flow of a non-Newtonian fluid over a vertical stretching sheet, Can J Appl Sci 2 (1), 202-215